The 2009 IEEE/RSJ International Conference on
Intelligent Robots and Systems
October 11-15, 2009 St. Louis, USA

3D Feature Based Mapping Towards Mobile Robots' Enhanced Performance in Rescue Missions

Paloma de la Puente, Diego Rodriguez-Losada, Alberto Valero and Fernando Matia

Abstract— **This paper presents a feature based 3D mapping approach with regard to obtaining compact models of semi-structured environments such as partially destroyed buildings where mobile robots are to carry out rescue activities. To gather the 3D data, we use a laser scanner, employing a nodding data acquisition system mounted on both real and simulated robots. Our segmentation algorithm comes up from the integration of computer vision techniques, allowing for a fast separation of points corresponding to different, not necessarily planar, surfaces. The subsequent extraction of geometrical features out of each region's points is done by means of least-squares fitting. A Maximum Incremental Probability algorithm formulated upon the Extended Kalman Filter provides 6D localization and produces a map of planar patches with a convex-hull based representation. Scenarios from the Unified System for Automation and Robot Simulation (USARSim), including world models from past RoboCup Rescue editions' arenas, have been utilized to conduct some of our experiments.**

I. INTRODUCTION

A growing trend towards focusing on the importance of building clear, easy to understand models of the environment is lately being observed in the mobile robotics research community. As pointed out by S. Lacroix [1], for most applications it is no use precisely solving the robot's localization problem if the map that is created is unrecognizable, confusing or too complicated. The importance of searching new models of representation is also pointed out in [1], where splines are used to avoid sticking to a particular geometry. In teleoperation tasks, and whenever human perception is involved, it is specially interesting to generate as meaningful and rich as possible maps. The new challenge is about dealing with this issue while taking into account the 3D nature of the world. Overcoming the limitations imposed by the 2D models is not only a key aspect regarding safe navigation but may also help to improve scene interpretation notably.

There exist three main representation techniques to accomplish the construction of 3D maps with mobile robots, namely raw data representation, occupancy grid representation and feature based representation.

Building 3D maps from raw data by applying scan-matching algorithms has thus far been the most popular solution. This approach is positively the most appropriate for outdoor poorly structured environments. [2], [3] employ the Iterative Closest Point (ICP) algorithm starting from an initial heuristic estimation and applying an off-line refinement method obtain good results with the robot Kurt3D. [4] presents a fast scan-matching implementation and an integration of probabilistic methods for 2D localization extended to the creation of compact 3D maps by using multi-resolution techniques adopted from the computer graphics literature. [5] also takes 2D scan-matching localization as the starting point to originate 3D maps of an abandoned mine. [6] proposes a robust scan-matching algorithm to build 3D point based maps of outdoor environments. [7] also uses the raw 3D point as the representation element to build 3D models of outdoor environments, distinguishing among several classes of points depending on their belonging to tree trunks or crowns,to the floor, etc. In [8], semantic information from point labeling is exploited to improve and accelerate the correspondences search process of the ICP.

As for the occupancy grid representation, its applicability within the 3D space is not very practical due to the high amount of available memory which it requires. In [9], however, an example for autonomous exploration is presented.

Some of the most popular solutions to the 2D Simultaneous Localization and Mapping (SLAM) problem are based upon the Extended Kalman Filter (EKF), whose standard equations can be found in [10]. EKF-SLAM's main advantage is its capability to explicitly maintain a complete posterior estimation in an incremental fashion at the expense of accepting that the noise in the odometry and exteroceptive measurements can be approximated by a normal distribution.

Moving on to the third dimension, nevertheless, few approaches are based on this EKF framework. The most significant contributions have been made by [11], [12], with the development of a 3D mapping system employing the infinite plane as a geometrical feature within the Symmetries and Perturbations Model (SpModel,[13]). Another method to build 3D maps through EKF-SLAM is the one proposed in [14] with the idea of creating maps of heterogeneous features by associating lines obtained from camera images to planes detected from 3D laser sensor data. In this work only the planes are integrated into the filter yet the objective of incorporating the lines is established as near to come work.

The feature based approach leads to compact representations with a high speed of execution and little memory consumption. Besides, it can be a means to filter some of the measurements' noise and establishes a basis to recognize objects or structures to reason upon at higher levels of cognition. Its main drawbacks are related to the loss of information and the difficulties intrinsic to the feature extraction process, as well as to the problems derived from the data association.

This work was partially funded by the Spanish Ministry of Science and Technology, DPI2007-66846- c02-01 and the Comunidad de Madrid

P. de la Puente, D. Rodriguez-Losada, A. Valero and F. Matia are with the Intelligent Control Group, Universidad Politecnica de Madrid, 28006 Madrid, Spain paloma.delapuente@upm.es

[1]Course lecture

[15],[9] address feature based map building by means of scan-matching and the imposition of global restrictions. The detected planes' location is estimated with an Estimation Maximization (EM) algorithm, including information about the main directions.

The benefits that 3D mapping can introduce in rescue robotics have not been much exploited. In the Robocup Rescue competition [16] very few teams have attempted to perform 3D mapping. In the Real Robots project the algorithms exposed in [8] have been successfully applied. Another group [17] has gone for employing a gravity sensor to measure the current orientation of the robot and then correct the position of a laser scanner so that it always remains horizontal. This approach is interesting to build high quality 2D maps and keep good localization results but it is not a good enough solution, for it does not avoid the risk of encountering obstacles that the sensor cannot detect. To the authors' knowledge, no team has ever used 3D mapping in the Virtual Robots initiative. Last year one single team (SPQR) gained enhanced situational awareness for the operator by making use of two laser rage finders to build elevation maps (2.5D).

The rules and settings for the 2009 competition are specially suited for 3D mapping. The context of the rescue mission is a gas explosion in a railway station, which will probably cause some robots to fall into the rails. The most relevant change with respect to previous years is the obligation to leave the robots in autonomous mode half of the mission time. During teleoperation control the user can avoid some obstacles on the ground thanks to camera images but when it is the autonomous operation mode that is active, that kind of objects must be somehow represented in the map. 3D mapping seems to be the natural option to tackle this issue.

The paper is organized as follows. Section 2 describes our 3D data acquisition system. In Section 3 we explain our segmentation algorithm and the fitting process, including the convex-hull representation of planar patches. Section 4 presents the Maximum Incremental Probability algorithm for localization and mapping. Section 5 accounts for experimental results we have obtained. Finally, Section 6 comprises our conclusions and future working lines.

II. 3D DATA ACQUISITION

Although there are some other means to obtain 3D data from the environment, up to now the laser range scanner is the most popular exteroceptive sensor in mobile robotics. [18] summarizes some of its main advantages and describes several alternatives to gather the 3D data. [19] also includes a comparison of methods.

Our system configuration is shown in Fig. 1. Our Pioneer 3AT robot Nemo is equipped with a SICK LMS200 laser device mounted on top of a servo pan-tilt unit (PowerCube Wrist 070, by Amtec Robotics). We obtain a 3D scan by varying the tilt angle at a constant speed.

A data server running on an onboard mini laptop computer sends synchronized updated information about odometry,

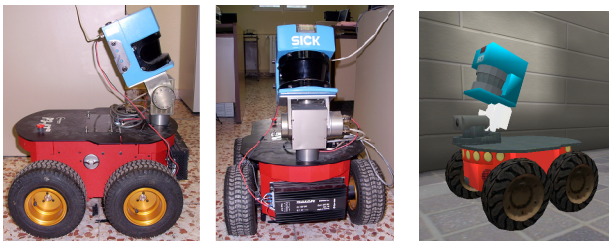

Fig. 1. Left:3D data acquisition system, mounted on our robot Nemo. Right: The USARSim Nemo's model we have built

PW70 and laser measurements at clients' cyclical requests within a capture procedure in a stop-scan-go manner.The port's baud rate for the laser scanner is set at 500 kb (using an external USB to 422 interface) so as to gain velocity and permit a good precision in the synchronization with the PW70. This is of utmost importance to avoid distortions when applying the relative transformations to calculate each point's cartesian 3D coordinates.

The simulated robot works in a slightly different way. Since the pan-tilt unit that is already available in USARSim [20] can receive action commands but does not provide the angular reading, we have implemented a step by step motor system that waits long enough for the command to be executed and then acquires the laser data, hence associated to the previously demanded tilt angular value. Our software uses the OpenRDK [21] framework.

III. SEGMENTATION AND FITTING

Segmentation undertakes the partition of a 3D point cloud into smaller subsets representing objects of interest (different surfaces, here). Points identified as part of the same region are allotted the same tag so that they can be treated as raw data of a sought-after feature.

To solve the 3D laser data segmentation problem we proposed a novel algorithm integrating vision-based techniques. For each 3D point, we select its neighborhood with an eight connectivity criterion and compute the residual of their least squares fitting to a plane model, which gives a quite good approximation of the local curvature [22]. After properly scaling the obtained values we create a range image, which as expected reveals higher values of the residuals at the different surfaces' boundaries. After applying several morphological operations, a floodfilling algorithm lets us uniquely color each large enough region and accordingly classify the points. An outline of the whole algorithm is presented in [18]. In order to totally rely on its robustness we have introduced a posterior checking stage to subdivide regions which eventually may not be correctly extracted due to the presence of not clear enough borders in the image. Comparing the angle between local normals, the number of under segmentation cases is significantly reduced while the computation time remains practically unaltered and the algorithm is still very fast (1 % of extra time required on average).

Once the points of a continuos individual surface are grouped together, a geometrical model can be extracted.

We employ the least-squares fitting method to obtain the representation parameters of planes, spheres and cylinders. The equations that we use are summarized in [18].

So as to better represent the actual extension of a planar patch, we determine the convex-hull of the points of each planar region resulting from the fitting process. The convex-hull of a set of 2D points is the smallest convex polygon with vertices belonging to the set that contains all the points in it. The algorithm we have used is the one presented in [23]. The points in the set which are vertices of its convex-hull are called the extreme points of the set. Being n the number of points in the set and h the number of extreme points in the set, the algorithm's computational cost is $O(nh)$.

IV. LOCALIZATION AND MAPPING

To deal with this problem in the 3D space, we have formulated a Maximum Probability algorithm based on the detected planes to correct the robot's 6D localization estimation and accordingly create the most probable complete map at each processing cycle.

Our state vector contains the six parameters that define the robot's position and orientation through the Euler roll, pitch and yaw angles around the global z axis, y axis and x axis, respectively, taking the initial configuration of the robot as the global reference frame. This vector is represented as $\mathbf{x}_R = [x_R, y_R, z_R, \phi_R, \theta_R, \psi_R]^T$. The state's covariance will be denoted as P.

A. Prediction

The odometry measurements are incremental for the shake of increased generality, so they are referred to the robot's local reference system. This input vector will be given by $\mathbf{u} = [u_x, u_y, u_z, u_\phi, u_\theta, u_\psi]$ at every moment; we omit the time subscripts to simplify the notation. The robot's encoders only provide values for u_x, u_y and u_ϕ. The other components are set to zero and the possible variations in the z_R, θ_R and ψ_R estimations are introduced on the grounds of the acquired observations (update stage). The standard deviation of those measurements is given a high value to account for the lack of information about those degrees of freedom, as proposed in [12], [19].

At each iteration k, the state's prediction is:

$$\tilde{\mathbf{x}}_{\mathbf{R_k}} = f(\mathbf{x_R}, \mathbf{u})_{\hat{\mathbf{x}}_{\mathbf{R_{k-1}}}, \mathbf{u_k}} = \hat{\mathbf{x}}_{\mathbf{R_{k-1}}} \oplus \mathbf{u}, \tag{1}$$

where the $\oplus$ operator corresponds to the composition of relative transformations in the 6D space, being it given by the location associated to the product of the homogeneous matrices defining both transformations. The noise in the odometry measurements is considered as gaussian white noise (as required to apply the EKF), and $\mathbf{u}$ is represented as $\mathbf{u} \sim N(\hat{\mathbf{u}}, Q)$.

The prediction of the state's covariance will be:

$$\tilde{P}_k = F_x \hat{P}_{k-1} F_x^T + F_u Q F_u^T, \tag{2}$$

with $F_x = \frac{\delta f}{\delta \mathbf{x_R}} \mid_{\hat{\mathbf{x}}_{\mathbf{R_{k-1}}}, \mathbf{u_k}} = J_{1\oplus}(\hat{\mathbf{x}}_{\mathbf{R_{k-1}}}, \mathbf{u_k})$ and $F_u = \frac{\delta f}{\delta \mathbf{u}} \mid_{\hat{\mathbf{x}}_{\mathbf{R_{k-1}}}, \mathbf{u_k}} = J_{2\oplus}(\hat{\mathbf{x}}_{\mathbf{R_{k-1}}}, \mathbf{u_k})$.

$J_{1\oplus}$ and $J_{2\oplus}$ represent the jacobian matrices of the composition of relative transformations $\oplus$ with respect to the first and the second components, respectively.

The algorithm is initiated with $\hat{x}_0 = 0, \hat{P}_0 = 0$.

B. Data Association and Update

The observed O_i planes obtained after the fitting process are related to the state and compared with those that are already in the map (the F_j planes) by means of the innovation vector. In our model we employ the implicit observation equation based version of the EKF:

$$\mathbf{h_{ij}} = B[\ominus \mathbf{x_{F_j}} \oplus \tilde{\mathbf{x}}_{\mathbf{R}} \oplus \mathbf{x_{O_i}}], \tag{3}$$

B is the so called *binding matrix* introduced by the SP-Model. It is used in order to only keep those components in the innovation vector which may actually mean a discrepancy between the O_i observed element and the F_j element in the map.

When dealing with planes, with a local reference frame defined by the coordinates of its center of gravity ($[ox, oy, oz]^T$) and the roll, pitch and yaw angles so that the local z axis coincides with the plane's normal, the B matrix comes to be [12]:

$$B = \begin{pmatrix} 0 & 0 & 1 & 0 & 0 & 0 \\ 0 & 0 & 0 & 0 & 1 & 0 \\ 0 & 0 & 0 & 0 & 0 & 1 \end{pmatrix}, \tag{4}$$

for infinite planes are invariant to translations along the local x, y axes and to rotations around the local z axis.

For the application of the EKF, the following jacobian matrices are employed:

$$H_{x_{ij}} = \frac{\delta \mathbf{h_{ij}}}{\delta \mathbf{x_R}} = B J_{2\oplus}(\ominus \mathbf{x_{F_j}}, \tilde{\mathbf{x}}_{\mathbf{R}} \oplus \mathbf{x_{O_i}}) J_{1\oplus}(\tilde{\mathbf{x}}_{\mathbf{R}}, \mathbf{x_{O_i}}) \tag{5}$$

$$H_{z_{ij}} = \frac{\delta \mathbf{h_{ij}}}{\delta \mathbf{x_O}} = B J_{2\oplus}(\ominus \mathbf{x_{F_j}}, \tilde{\mathbf{x}}_{\mathbf{R}} \oplus \mathbf{x_{O_i}}) J_{2\oplus}(\tilde{\mathbf{x}}_{\mathbf{R}}, \mathbf{x_{O_i}}) \tag{6}$$

This two matrices' dimensions are $3x6$. For the $H_{z_{ij}}$ matrices, we only store the third, fifth and sixth columns. The covariance matrix of an individual observation is:

$$S_{ij} = H_{x_{ij}} \tilde{P}_k H_{x_{ij}}^T + H_{z_{ij}} R_{ij} H_{z_{ij}}^T, \tag{7}$$

being R_{ij} the covariance matrix of the noise in the planes extracted from the laser measurements. Only the significant parameters oz, θ and ψ are considered; R_{ij} is a $3x3$ matrix.

This way the squared Mahalanobis distance between the observation and the map object can be computed as usual:

$$d_M^2 = \mathbf{h_{ij}}^T S_{ij}^{-1} \mathbf{h_{ij}} \tag{8}$$

The planes that cannot be associated to any feature in the map are added to it after applying the composition of both transformations. The vectors and matrices corresponding to an accepted association are denoted as h_i, H_{x_i} and H_{z_i}, to be used afterwards.

For the correction we employ the joint matrices containing the information from all valid associations:

$$\mathbf{h_k} = \begin{pmatrix} \mathbf{h_1} \\ \mathbf{h_2} \\ \vdots \\ \mathbf{h_N} \end{pmatrix} \tag{9}$$

$$H_{x_k} = \begin{pmatrix} H_{x_1} \\ H_{x_2} \\ \vdots \\ H_{x_N} \end{pmatrix}, H_{z_k} = \begin{pmatrix} H_{z_1} & & & \\ & H_{z_2} & & \\ & & \ddots & \\ & & & H_{z_N} \end{pmatrix} \tag{10}$$

The joint covariances matrix for all the innovations corresponding to the accepted associations is given by:

$$S_k = H_{x_k} \tilde{P}_k H_{x_k}^T + H_{z_k} R H_{z_k}^T, \tag{11}$$

where R is the block diagonal matrix composed of as many R_{ij} matrices as associations are made.

The system's Kalman gain $6x3N$ matrix will be:

$$W = \tilde{P}_k H_{x_k}^T S_k^{-1} \tag{12}$$

Finally, the corrected values for the robot's pose and its covariance are obtained from the prediction by:

$$\hat{\mathbf{x}}_{\mathbf{R_k}} = \tilde{\mathbf{x}}_{\mathbf{R_k}} - W\mathbf{h_k} \tag{13}$$

$$\hat{P}_k = (I_{6x6} - W H_{x_k}) \tilde{P}_k \tag{14}$$

V. FIELD OF APPLICATION

As we have previously explained, we are working on full 3D localization and mapping. Localization using full 3D data has the advantage of incorporating much more data than usual SLAM solutions, which only work in 2D. This allows our robot to be localized not only considering obstacles at the laser sensor's height, which may become very useful in very large indoor areas and outdoor scenarios.

We would also like to outline two major advantages derived from using 3D maps.

- **Autonomous Path planning and Navigation**
  Autonomous Path Planning and Navigation techniques are responsible of moving the robot towards a target pose. They are usually implemented using the well-known two-level decomposition, in which a global algorithm computes a path towards the goal, using a simplified model of the environment (path planning); this path is followed by a local algorithm (navigation), that generates the motion commands to steer the robot to the current goal [24]. As obstacles that are below the laser cannot be seen, autonomous navigation with 2D maps is doomed to failure in a lot of environments. Examples of these environments are office environments or outdoor urban environments with the presence of pavements' curbs and other obstacles, the kind of environments often found in rescue and many other service robotics applications.
- **Operator Situational Awareness**
  When a human operator guides a robot using a Graphical User Interface (GUI), he or she must have a proper Situational Awareness (SA). The SA provided by interfaces has been regarded in the literature as one of the more relevant aspects to be considered for the evaluation of their respective usefulness [25][26][27][28]. In [26] and [29] the elevation of obstacles in a 2D map yields a pseudo 3D-environment. In [25] and [26] it is shown that with a point of view located beside the robots, a 3D view of the environment enhances the operator's SA. Anyway, the operator may be confused, because what they perceive as 3D is not real 3D, and obstacles that are supposed to be in the map are not there. For it to be really useful, a 3D map should actually provide full 3D info.

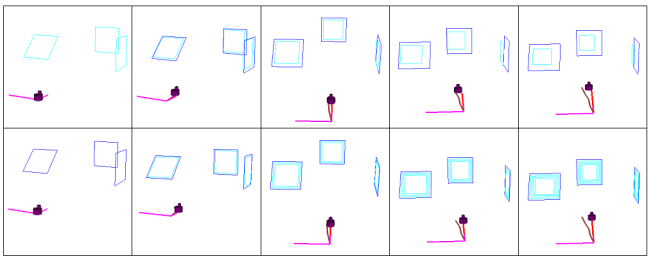

Fig. 2. Localization based on the observation of three planes. The planes depicted in light blue correspond to the observations, the planes depicted in dark blue are the objects in the map. The first row represents the prediction stage of the algorithm and the second row represents the situation after the update stage. The brown path is odometry and the red path is the correction.

VI. EXPERIMENTS AND RESULTS

As previously mentioned, experiments have been carried out in both real and simulated environments.

To capture the 3D data, the laser is tilted from -25 degrees (upwards looking) to 30 degrees (downwards looking) at a constant speed of 0.05 rad/s, which results in a 70x181 matrix of measurements. When gathering data with the simulated robot, the tilt increment is fixed at 0.25 degrees to obtain a good level of continuity in the floor and ceiling data. Therefore, the number of 2D scans in this case is 220 instead of 70. We process the central 131 columns so as to avoid problems caused by the points being too near one from each other at the extreme lateral angles of the view area. The segmentation process takes about 1 second per scene.Our code has been developed in C++ using the OpenCv libraries.

The localization and mapping algorithm was initially tested with simple sets of observations, one example consisting of three planes including a not vertical one. The theoretical movement was a pure translation along the x axis' direction. Noise of 0.3m standard deviation in the x and y components was introduced into the odometry data. The results are shown in Fig. 2 and Table I.

TABLE I

LOCALIZATION RESULTS

	Odometry Pose	Predicted Pose	Corrected Pose
0	$[0,0,0,0,0,0]^T$	$[0,0,0,0,0,0]^T$	$[0,0,0,0,0,0]^T$
1	$[1.169,0.169,0,0,0,0]^T$	$[1.169,0.169,0,0,0,0]^T$	$[1,0.002,-9\cdot10^{-6},-6\cdot10^{-4},-2.15\cdot10^{-11},3.2\cdot10^{-16}]^T$
2	$[2.227,0.227,0,0,0,0]^T$	$[2.058,0.06,0,-6\cdot10^{-4},0,-3.3\cdot10^{-8}]^T$	$[2,0.0015,4\cdot10^{-6},-5\cdot10^{-4},7\cdot10^{-12},-2.5\cdot10^{-11}]^T$
3	$[3.470,0.470,0,0,0,0]^T$	$[3.243,0.241,0.000,-5\cdot10^{-4},0,0]^T$	$[3,0.001,1.9,\cdot10^{-6},-5\cdot10^{-4},2\cdot10^{-12},-2\cdot10^{-11}]^T$
4	$[4.645,0.645,0,0,0,0]^T$	$[4.176,0.176,0,-5\cdot10^{-4},0,0]^T$	$[4,5\cdot10^{-4},6.7\cdot10^{-6},-5\cdot10^{-4},7\cdot10^{-12},-2.5\cdot10^{-11}]^T$

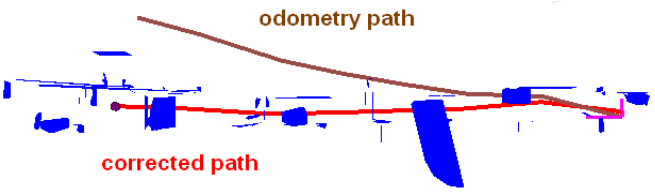

Fig. 3. View from above of a 3D map built at our laboratory

The whole 3D mapping system has been thoroughly tested in more cluttered and complicated environments. Fig. 3 shows the view from above of a map built at our laboratory. The map is made up of 110 elements, while the number of accepted associations is 22. The localization results are similar to those provided by an efficient 2D feature based SLAM algorithm [30],[31](See Fig. 4). The 3D map contains much more information and can be better interpreted by a human (Fig. 5).Fig. 6 reflects the compactness and expressiveness of a 3D map of a USARSim setting. Fig. 7 is its 2D counterpart, generated with the algorithm presented in [32]. The room marked with an X is depicted in more detail in Fig. 8. The ramps can hardly be identified as such in the 2D map.Fig. 9 shows another example of a USARSim rescue environment modeled in 3D, including the images generated throughout the segmentation process. The 2D map of the same place does not correctly represent the obstacles in the scene, so it is not very realistic either (Fig. 10).

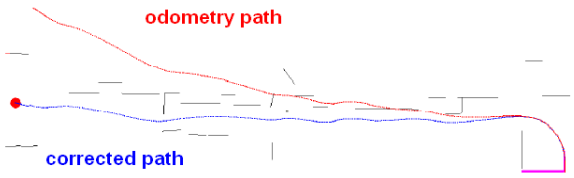

Fig. 4. 2D map of our laboratory [31]

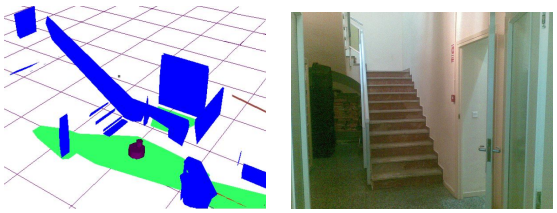

Fig. 5. Left: detailed scene of the 3D map of our laboratory. Right: the actual environment.

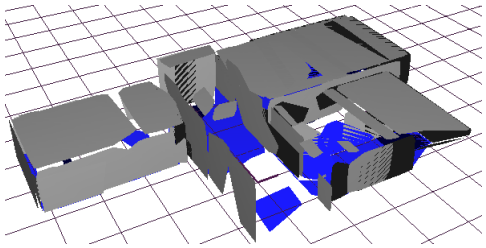

Fig. 6. 3D map of a USARSim scenario for validation tests

VII. CONCLUSIONS AND FUTURE WORK

We have put forward a set of algorithms to build 3D maps with mobile robots, emphasizing their potential to improve autonomous navigation and the operators' SA, especially in rescue oriented activities, in which we deem both aspects play a vital role. We strive for fast algorithms that allow for a real-time compact and meaningful representation. Experiments to strengthen our point have been conducted in real and USARSim Rescue environments.

As future work, we aim to add textures to the maps to make them more appealing to the human eye. We also plan to integrate the 3D information into a 2D occupancy grid map to be actually used for navigation in the RoboCup Virtual Robots 2009 competition. As longer term goal we seek creating higher level models of representation to incorporate topological information to the maps and reason upon different hypothesis so that more meaningful and consistent

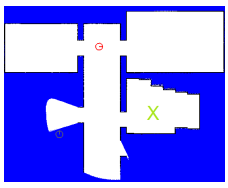

Fig. 7. 2D map of the environment in Fig. 6. The 2D SLAM algorithm employed is described in [32]. The marked room is depicted in Fig. 8

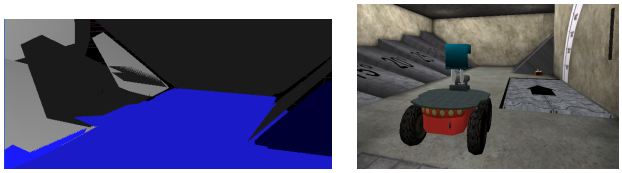

Fig. 8. Left: detailed scene of the 3D map showed in Fig. 6. Right: the USARSim scene

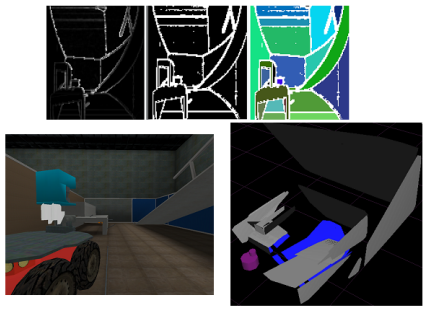

Fig. 9. 3D model of a USARSim rescue environment

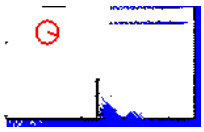

Fig. 10. 2D map of the scene in Fig. 9

3D maps can be built.

REFERENCES

[1] L. Pedraza, G. Dissanayake, J. Valls Mir, D. Rodriguez-Losada, and F. Mata, "BS-SLAM: Shaping the world," in *Proc. Robotics: Science and Systems (RSS'07)*, Atlanta, GA, USA, June 2007. [Online]. Available: http://www.roboticsproceedings.org/rss03/p22.html

[2] A. Nuchter, K. Lingemann, J. Hertzberg, and H. Surmann, "6D SLAM - 3D mapping outdoor environments," *Journal of Field Robotics*, no. 24, pp. 699–722, 2007.

[3] A. Nuchter, K. Lingemann, and J. Hertzberg, "6D SLAM with Kurt 3D," *Robotics Today*, vol. 20, no. 1, 2007.

[4] S. Thrun, W. Burgard, and D. Fox., "A real-time algorithm for mobile robot mapping with applications to multi-robot and 3D mapping." in *Proc. IEEE International Conference on Robotics and Automation (ICRA'00)*, 2000.

[5] S. Thrun, D. Hahnel, D. Ferguson, M. Montemerlo, R. Triebel, W. Burgard, C. Baker, Z. Omohundro, S. Thayer, and W. Whittaker, "A system for volumetric robotic mapping of abandoned mines," in *Proc. IEEE International Conference on Robotics and Automation (ICRA'03)*, 2003.

[6] D. M. Cole and P. M. Newman, "Using laser range data for 3D SLAM in outdoor environments," in *Proc. IEEE International Conference on Robotics and Automation (ICRA'06)*, 2006.

[7] C. Brenneke, O. Wulf, and B. Wagner, "Using 3d laser range data for slam in outdoor environments," in *IEEEWRSI Intl. Conference on Intelligent Robots and Systems*, 2003.

[8] A. Nuchter, O. Wulf, K. Lingemann, J. Hertzberg, B. Wagner, and H. Surmann, "3D Mapping with semantic knowledge," in *RoboCup International Symposium*, 2005.

[9] R. Triebel, "Three-dimensional perception for mobile robots," Ph.D. dissertation, Albert-Ludwigs-Universitat Freiburg, 2007.

[10] J. D. Schutter, J. D. Geeter, T. Lefebvre, and H. Bruyninckx, *Kalman Filters: A Tutorial*, 1999.

[11] J. Weingarten and R. Siegwart, "EKF-based 3D SLAM for structured environment reconstruction," in *Proc. IEEE International Conference on Intelligent Robots and Systems (IROS'05)*, 2005.

[12] J.Weingarten and R.Siegwart, "3D SLAM using planar segments," in *Proc. IEEE International Conference on Intelligent Robots and Systems (IROS'06)*, 2006.

[13] J. A. Castellanos, M. M. Montiel, J. Neira, and J. Tardos, "The SPmap: A probabilistic framework for simultaneous localization and map building," *IEEE Transactions on Robotics and Automation*, vol. 15, pp. 948–952, 1999.

[14] A. Zureiki, M. Devy, and R. Chatila, "SLAM and data fusion from visual landmarks and 3D planes," in *Proc. 17th IFAC World Congress*, 2008.

[15] R. Triebel, W. Burgard, and F. Dellaert, "Using hierarchical EM to extract planes from 3D range scans," in *Proc. International Conference on Robotics and Automation(ICRA'05)*, 2005.

[16] (2009) The RoboCup website. [Online]. Available: http://www.robocuprescue.org/

[17] J. Pellenz and D. Paulus, "Mapping and map scoring at the RoboCupRescue competition," in *Quantitative Performance Evaluation of Navigation Solutions for Mobile Robots (RSS'08, Workshop CD)*, 2008.

[18] P. de la Puente, D. Rodríguez-Losada, R. López, and F. Matía, "Extraction of geometrical features in 3D environments for service robotic applications," in *Proc. 3rd. International Workshop on Hybrid Artificial Intelligent Systems (HAIS'08)*, ser. LNCS, A. A. P. W. Corchado, E., Ed., vol. 5271. Springer-Verlag, 2008, pp. 441–450.

[19] A. Nuchter, *3D Robotic Mapping*, ser. Springer Tracts in Advanced Robotics (STAR). Springer Verlag, 2009.

[20] (2009) The USARSim website. [Online]. Available: http://usarsim.sourceforge.net/

[21] (2009) The OpenRDK website. [Online]. Available: http://openrdk.sourceforge.net/

[22] T. Rabbani, F. A. van den Heuvel, and G. Vosselman, "Segmentation of point clouds using smoothness constraint," in *ISPRS Commission V Symposium 'Image Engineering and Vision Metrology'*, 2006.

[23] A. Bykat, "Convex hull of a finite set of points in two dimensions," *Inform. Process. Lett.*, vol. 7, pp. 296–298, 1978.

[24] D. Calisi, A. Farinelli, L. Iocchi, and D. Nardi, "Multi-objective exploration and search for autonomous rescue robots," *Journal of Field Robotics, Special Issue on Quantitative Performance Evaluation of Robotic and Intelligent Systems*, vol. 24, pp. 763–777, August - September 2007.

[25] J. L. Drury, B. Keyes, and H. A. Yanco, "LASSOing HRI: analyzing situation awareness in map-centric and video-centric interfaces," in *Proc. 2nd ACM SIGCHI/SIGART Conference on Human-Robot Interaction*, 2007, pp. 279 – 286.

[26] C. W. Nielsen and M. A. Goodrich, "Comparing the usefulness of video and map information in navigation tasks," in *Proc. 1st ACM SIGCHI/SIGART Conference on Human-Robot Interaction, (HRI'06)*, 2006, pp. 95–101.

[27] D. R. Olsen and M. A. Goodrich, "Metrics for evaluating human-robot interactions," in *Proc. PERMIS'03*, 2003.

[28] J. Scholtz, J. Young, J. L. Drury, and H. A. Yanco, "Evaluation of human-robot interaction awareness in search and rescue," in *Proc. IEEE International Conference on Robotics and Automation (ICRA'04)*, vol. 3. IEEE, May 2004, pp. 2327 – 2332.

[29] A. Valero, G. Randelli, C. Saracini, F. Botta, and M. Mecella, "The advantage of mobility, mobile tele-operation for mobile robots," in *Proc. AISB-HRI Symposium "New Frontiers in Human - Robot Interaction (To appear)*, March 2009.

[30] D. Rodríguez-Losada, F. Matía, A. Jiménez, R. Galán, and G. Lacey, "Implementing map based navigation in guido, the robotic smartwalker," in *Proc. IEEE International Conference on Robotics and Automation (ICRA'05)*, 2005.

[31] D. Rodríguez-Losada, "Slam geométrico en tiempo real para robots móviles en interiores basado en EKF," Ph.D. dissertation, Universidad Politécnica de Madrid, ETSI Industriales, 2004.

[32] G. Grisetti, C. Stachniss, and W. Burgard, "Improved techniques for grid mapping with rao-blackwellized particle filters," *IEEE Transactions on Robotics*, 2006.